IIETA International Information and Engineering Technology Association
Advancing the World of Information and Engineering

European Journal of Electrical Engineering
Vol. 24, No. 1, February, 2022, pp. 55-65
Journal homepage: http://iieta.org/journals/ejee

EPLL Control Technique Optimum Controller Gains to Control Voltage and Frequency in Standalone Wind Energy Conversion System

Bochu Subhash[1*], Veramalla Rajagopal[2]

[1] Department of Electrical and Electronics Engineering, JNTU Hyderabad, Hyderabad 500085, India
[2] Department of Electrical and Electronics Engineering, Kakatiya Institute of Technology and Science, Warangal 506015, India

Corresponding Author Email: subhashbochu@gmail.com

https://doi.org/10.18280/ejee.240108

Received: 3 February 2022
Accepted: 22 February 2022

Keywords:
standalone wind energy conversion system (SWECS), induction generator (IG), battery energy storage system (BESS), PI controller, voltage and frequency controller (VFC), zigzag transformer, particle swam optimization (PSO)

ABSTRACT

This study describes how to regulate the frequency and terminal voltage of a freestanding wind energy conversion system using an Enhanced Phase Locked Loop (EPLL)-based strategy to supply power to varied loads regardless of wind speed. In a standalone wind turbine energy conversion system, the EPLL control scheme extracts the reference source currents (SWECS). The control algorithm employs two proportional-integral (PI) controllers to create the active and reactive power components of the consumers' load currents, estimate reference source currents, and connect the zigzag transformer to PCC with VSC for neutral current compensation. To obtain optimal PI controller gains and most-suited settings to apply to SWECS, optimization approaches are used. The control algorithm is the most significant aspect of the system, and the speed with which it calculates, evaluates, and guesstimates determines the generation of source currents based on the algorithm's ideal controller PI gains. By properly estimating source currents, the EPLL control method improves dynamics and power quality issues, and the optimization technique is employed to acquire the gains of PI controllers. The proposed system employs the EPLL algorithm on a three-phase, four-wire system with changing loads to achieve ideal total harmonic distortion of source currents and voltages on the PCC, as defined by IEEE-519 standards. A battery energy storage device coupled to the VSC dc link keeps the load's necessary power constant. If the generator output exceeds the consumer demand, the excess power is delivered to BESS for temporary storage. When consumer demand exceeds generated power, a BESS delivers deficit power to the load, which adjusts and the frequency under various load conditions. The suggested system simulated results were tested with 3-phase 4-wire for harmonics reduction, load balancing, neutral wire current compensation, frequency and voltage control using MATLAB / Simulink.

1. INTRODUCTION

Now the whole world is facing today environmental degradation due to intensifying fossil fuels usage and conventional natural resources exploitation along with growing different consumer's power demands and significant transmission cost its losses and power generation to remote regions are great challenges. The great awareness regarding environmental issues, government initiatives lead us to utilization renewable resources and the main objective, importance, ground level targets are with operational design model and electro-mechanics for power generation with non-conventional resources are described. The technocrats, power providers focused on the uppermost consumer demand along with maximum electricity price and feeding largest generated electricity power to existed utility grid with increased the system efficiency and power reliability storage requirements [1]. Nowadays Remote area power supply (RAPS) patterns, schemes are attractive, more demanding for remote, hill areas and islands. In absence of main grid, RAPS system design and operation is more challenging in power generation supply system with distinctive nature and described unexpected voltage and frequency unallowable limits due to less(X/R) ratios, deficiency of reactive power support and low damping, therefore the voltage and frequency control is the prime important aspects which to be controlled whenever we design and implement RAPS systems [2, 3]. In the last decade, the entire world's many engineers concentrated and put their attention on wind energy conversion systems due to environmentally friendly and playing key role in producing the electrical power according to increased load demand from rural, hilly areas to high density populated urban areas, domestic consumer, industrial, agricultural demand which huge gap between generation and consumer demand overcoming by wind energy conversion systems which can be advisable plans for remote, isolated areas and islands and stand-alone wind energy generation is the one of the most demanded resources among Non-Conventional generation power systems, used for isolated consumer loads as well [4]. Since from last decades, the worldwide green energy source is a substantial significant effect on SWECS growth in wind energy generation from 19902 GW to present global installed capacity reached about 100 GW and future predictable growth to 1000 GW by 2025 and wind energy among several renewable energy resources expressed as rapid emergent energy industry in the electricity market [5].

Gowtham et al. [6] stated that the electrical engineers are resolved ground technical issues for smooth effective

synchronization of wind power plants to existing grid with worthy and efficient power supply to remote, hill area load consumers who are away from central grid but still the enormous availability, huge wind energy potential remains untapped and unutilized to till today. Since from three decade period, developed, designed, and erected different wind turbine technologies strategies as fixed speed, variable speed, and circuit topology for power generation with a low economical and variable wind speed technology is best remarkable in SWECS to regulate good voltage and frequency parameters as compared to constant wind speed technology [7, 8]. Rezkallah et al. [9] among the different wind turbine technologies based on design factor available for wind energy conversion systems, the supreme extensively used machines are DFIG and IG which are most advanced for remote wind generation due to their inheritance capabilities and induction generator (IG) is one best chosen due to it merit of decreased mechanical stress and optimal power capture due to varying wind speed operation by Xu et al. [10]. As per the load demand–generation mismatch, an energy storage device is introduced into power system to provide upgraded security and performance and also due to its high energy density levels of battery storage device is chosen. Wang et al. [11] recognized as best option among various energy storage machineries like superconducting magnetic energy storage, super capacitors and flywheels etc., for standalone wind power application operations to satisfy required power supply with optimal rated voltage and frequency control and cost perspective sizeable battery is not economical. Singh and Rajagopal [12] described RAPS with battery system load control coordination environment with great research attention. The battery machinery main aim is to deliver continual supply to inaccessible consumers from SWECS and standardize the voltage, control reactive power, stabilize system voltages, sustain dc capacitor voltage endured constant in Refs. [13, 14]. Karbouj and Rather 15] discussed and recommended different algorithms like Icosφ, ATILTS, SRF, PB, etc. are to regulate wind generator frequency, terminal voltage and set to maintained load leveling, load balancing, neutral current compensating. Tanaka et al. [16] detailed the improvement of the power issues by eliminating the harmonic in SWECS and raised anxieties about power quality are embattled in harmonics reduction, minimized power losses, and are enhanced purely sinusoidal waveforms of voltage and current components. Kasal and Singh [17] expressed the main objective and merit of usage the zig-zag transformer to alleviate moderate zero-sequence currents and triplen harmonics within primary winding itself with reduced VSC KVA rating and neutral wire current is compensated, secondary winding liberated from zero-sequence currents and also zig-zag winding transformer operation for regulating the voltage and system frequency constant in turn active power controls. Sharma and Singh [18] proposed EPLL algorithm control scheme main feature is used to generate basic reference source currents easily and accurately and used to extract the essential 3 phase load component currents, frequency approximation at PCC voltages. The voltage and frequency controller (VFC) by EPLL technique in SWECS with an inaccessible induction generator (IG) for 3-phase 4-wire loads and EPLL used for quickly extracting basic reference load voltages to minimize the PQ issues and VFC is for reactive component compensation, load current, regulating terminal voltage, frequency through the variable loads with all atmospheric wind conditions and same SPLL strategy also has computational time less and extraordinary estimation accuracy for estimate the reference load voltages, currents results are validated according to the studies [19, 20]. The main presentation and usage of particle swarm optimization (PSO) to bring harmony in control SWECS parameters and is employed to obtain the optimally regulated the tuned control parameters with overall global best of the system along with rapid fast efficient convergence capabilities for optimum fitness in order to enhance the frequency, voltage profile within frame limit with reduced real active power losses and wind system operations, security constraints and solving the problems [21, 22]. Singh and Rajagopal [23] emphasized on frequency and voltage control of small hydro power generation with six leg voltage source converters. The paper dealt with least mean square control strategy without any filters. The experts are explained and pronounced about the innovative Dragonfly, ALO algorithms with superiority Services with optimizing high level efficiency various policies to edifying refining overall system performance in terms of harmonics eradication, voltage regulation, load balanced and neutral wire current compensation [24, 25].

The control algorithm is the heart of the SWECS to improve power quality. There is a need for a control algorithm, which is quick to estimate the reference source currents. The control algorithm has two proportional and integral controllers which plays an important role to improve the dynamics of the system. The mathematical model control algorithm applied to SWECS system is expressed in Section III and Section IV discussed about standalone wind energy conversion system design and developed its various components like wind turbine technology, generator setup, battery storage element system etc. Each system components and associated control optimization controller gains with SWECS is addressed following Section V. Simulated results are demonstrated under varying winds and consumer load conditions were furnished VI Section. Conclusions are specified, provided in VII Section. The various factors of the standalone wind power generation system's voltage and frequency parameters are maintained constant with heuristic techniques with the EPLL algorithm. Among the available techniques, the paper dealt with a distinctive and advanced PSO techniques to be optimized the necessary PI controller gains to solve the problems in SWECS and evaluated results was presented with the proposed system simulation by EPLL algorithm with MATLAB Simulink toolboxes.

2. SYSTEM CONFIGURATION AND PRINCIPLE OF OPERATION

The speedy development in power engineering, communication and world technology has forced the engineers to think to have major utilization of standalone wind energy among renewable energy resources with innovative control techniques. The Kinetic Energy (KE) =1/2mVb3Aρ converted in to mechanical energy is used to revolve wind-generator set in turn the power output is extracted from the generator terminals which from small kW to Few MW power for the remote/urban householders in 2-5 kW to MW, the SWECS surplus power feeding existed grid and also supply remote area consumer demand as per the needs. It is very beneficial, useful to rural, interior consumers, remote consumers who are away from the grid, not connected. SWECS frequency is well-organized by altering turbine blade pitch angle for preserve

turbine same swiftness regardless of wind velocity with modeled circuit block diagram is demonstrated regarding the SWECS controller and rural power loads who are not coupled with main grid.

The Figure 1 demonstrate the whole off grid SWECS with various components like wind turbine-induction generator set, excitation Delta connected capacitor bank with linear/non-linear, balanced/unbalanced and dynamic power loads with proposed controller. The wind turbine has a fixed-pitch angle with variable-speed is coupled through an appropriate step-up gear box to 3Ø, 50 Hz, 4-pole, 415 V, 7.5 kW rated capacity IG with a delta (Δ) connected 8 KVAR capacitor bank across generator which is operated under 10 m/s wind speed to feed various consumer loads and build rated terminal voltage, frequency which are maintained within optimal values by VF controller based VSC, BESS via inter-facing inductor to filter harmonics and neutral current nullify by zigzag transformer during operation, no load condition of SWECS.

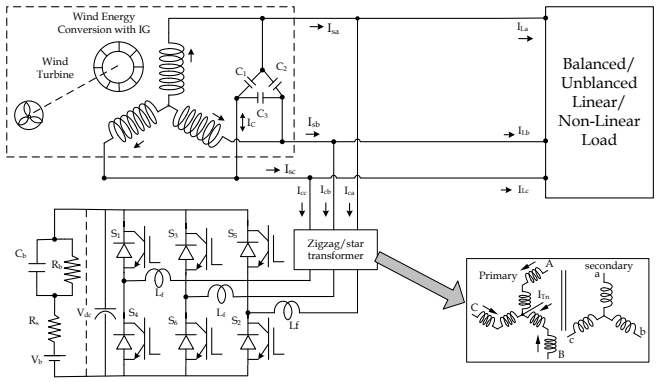

Figure 1. Schematic line diagram of standalone wind conversion system

The proposed VF controller consists 3-Ø insulated gate bipolar junction transistor (IGBT) based VSC, BESS, dc link on PCC and two IGBTs on each leg which common point connected each generator bus phase with an individual via inter-facing inductor. A ripple filter is developed, designed to eliminate terminal voltages high frequency harmonics. At no-load or specific load, producing, building the rated voltage by 3 phase delta-connected shunt excitation capacitor across generator terminals while the controller will develop the needed additional reactive power demand support for rated voltage regulation. Under various electrical and mechanical vibrant conditions magnitude of generated voltage and frequency to be controlled with bidirectional flow capabilities of the proposed controller and system frequency directly depends on accessibility, availability of wind input power and consumer demand power. The BESS is designed, technologically advanced as a 6-hour standby with its kVA rating which is almost equal to generator kVA rating in order to meet a max consumer load demand of two fold of generator kVA, 3-Ø 4-wire consumer loads are connected to generator neutral terminal from zigzag transformer which serves the neutral current compensation, tripled harmonics elimination in turn reduces the VSC rating in KVA.

It is necessity to study the VFC performance with 1-Ø loads for remote village electrification and 3-Ø 4-wire is developed in SWECS. The proposed SWECS working principle is with fixed speed operation of IG irrespective wind speed deviation or consumer loads variation. When large wind speeds or decreased consumer loads, the left-overpower stored in BESS to keep frequency constant. In same way when low wind speeds or increased consumer loads, the deficit power delivers by BESS to maintain frequency constant and frequency regulation took place active power exchange under changing wind speed/loads. The BESS stores the power if SWECS frequency beyond reference fit value and provides insufficiency power if SWECS frequency under rated values. System terminal voltage is controlled, regulated as per the need through varying the field winding current by a programmed voltage regulator and by consumer reactive power demand provided, supplied through VSC when application of loads. Implementation of the VFC needs a suitable choice of BESS, VSC, interfacing inductors DC link and circuits to detect input signal, driver circuits for output signal. The proposed EPLL-based control algorithm is implemented, evaluated and executed for SWECS. The large-frequency level harmonics signals from system terminal voltage are eradicated, eliminated by using designed filter. At zero pitch angles Generator output fluctuating varying wind speeds in turn changed in turbine speed and the characteristics curves with wind speeds of wind turbine-generator power are showed in Figure 2.

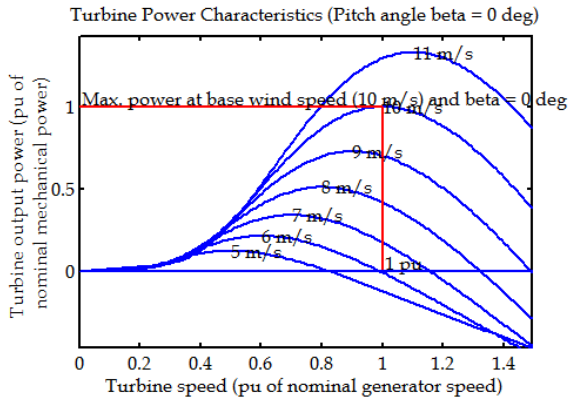

Figure 2. Schematic wind power- speed characteristic

3. CONTROL ALGORITHM

The Figure 3 symbolizes the main control algorithm block diagram which is to guesstimate the recommended control algorithm which make used for VFC and it performs and makes the various operating parameters through load leveling, load balancing, neutral wire current compensation, harmonic eradication. For the frequency regulation, the controller delivers or absorbs active power from VSC on PCC BESS. System voltage control, the controller deliveries, captivates the reference source currents in SWECS.

In the EPLL control algorithm, at PCC source phase v_{sa}, v_{sb}, v_{sc}, i_{sa}, i_{sb}, i_{sc}, voltages, currents, system load currents i_{La}, i_{Lb}, i_{Lc} along with v_{dc} dc-bus voltage utilization in order to take out of i^*_{sa}, i^*_{sb}, i^*_{sc} reference currents to VFC in wind system. In the algorithm mathematical equations are used to estimate the several operating control signals, which are explained in following passages.

In order to sense phase and frequency, a phase locked loop (PLL) used in SWECS to generate a harmonized, synchronized appropriate output signal and it works on a control feedback loop towards attain harmonization. Basic conventional construction of PLL to sense the inaccuracy signal error (e) created, formed by the phase detection is

proportional to input and output PLL phase difference signal. In a loop, the error signal is processed further filtered to decrease input error signals and finally voltage controlled oscillator to yield frequency and output phase. Many PLL techniques referred from the collected literature works like Synchronous Frame (SFPLL), PQPLL, SSIPLL (Sinusoidal Signal Integrator), DOSGI (Double Second Order Generalized Integrator), EPLL (Enhanced phase locked loop), QPLL etc. [26]. The main drawback of Conventional PLL unable to withdraw take away double frequency ripple from input signal and due to the unbalanced signal, twofold frequency factor can be diminished or reduced by the filter at the cost time delay. For the above reason EPLL algorithm is conversed below.

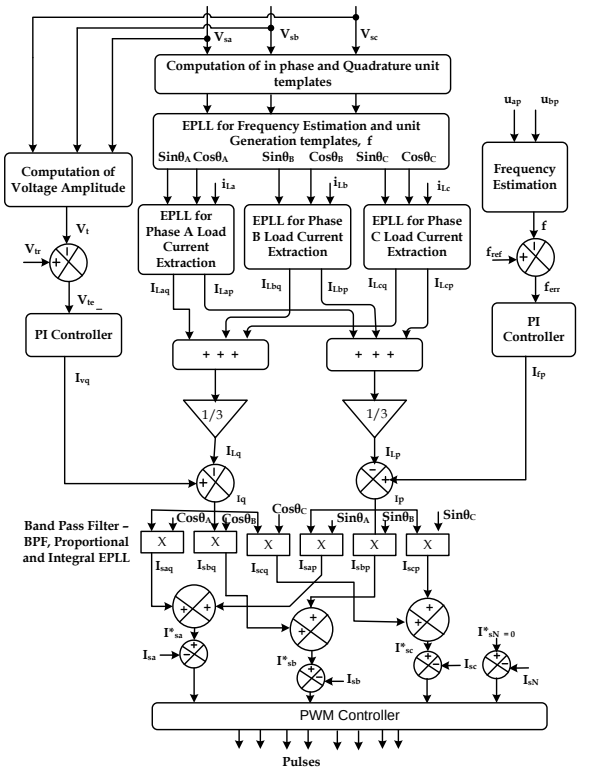

Figure 3. Control algorithm

3.1 The estimation of an average fundamental active, reactive components and unit voltage templates

Figure 4 described about the EPLL for estimation and extraction of fundamental active, reactive components, voltage magnitudes are evaluated and the 3-Ø system phase voltages are detected at PCC as v_a, v_b and v_c. Each singular phase voltages divided by V_t terminal voltages in order to get units amplitude along phase angle actual phase voltages which are divided in two as In phase components u_{pa}, u_{pb} and u_{pc} and Quadrature components u_{qa}, u_{qb} and u_{qc} respectively with phase a, b and c, source voltages v_{sa}, v_{sb},v_{sc} and amplitude terminal voltage V_t is determined by means of:

$$[V_t] = \sqrt{\frac{2}{3}\left(v_{sa}^2 + v_{sb}^2 + v_{sc}^2\right)} \qquad (1)$$

In-phase unit voltage amplitude templates along with phase voltages w_{ap}, w_{bp}, w_{cp} are forecast as:

$$\left[w_{ap}\right] = \left\{\frac{v_{sa}}{V_t}\right\}; \left[w_{bp}\right] = \left\{\frac{v_{sb}}{V_t}\right\}; \left[w_{cp}\right] = \left\{\frac{v_{sc}}{V_t}\right\} \qquad (2)$$

In the similar way, quadrature unit patterns w_{qa}, $w_{qb,}w_{qc}$ are calculated from below expressions.

$$\begin{aligned} \left[w_{aq}\right] &= \left[\left(-w_{bp} + w_{cp}\right)/\sqrt{3}\right] \\ \left[w_{bq}\right] &= \left[\left(3w_{ap} + w_{bp} - w_{cp}\right)/2\sqrt{3}\right] \\ \left[w_{cq}\right] &= \left[\left(-3w_{ap} + w_{bp} - w_{cp}\right)/\left(2\sqrt{3}\right)\right] \end{aligned} \qquad (3)$$

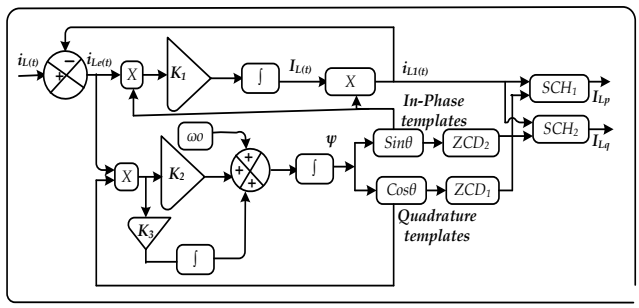

Figure 4. EPLL extraction of Active, Reactive component amplitudes Load current

In Figure 4 diagram of EPLL algorithm for extract the reactive and active power components of load current designed for each specific phase A or B, phase C. Basic ultimate load current iL1(t) always in phase with the iL(t) input signal, its explorations at a convinced particular phase angle with reference sinθ pattern. Therefore, in order to extract iL1 basic fundamental load current active power component amplitude is in phase with corresponding supply voltage, the ZCD1 zero crossing detectors used with cosθ template pattern with 90 leading from sinθ pattern. Therefore, at a peak of sinθ pattern a trigger pulse provided by ZCD1 and a sample-and-hold circuit SHC1 used with iL1(t) as an input signal need to get trigger pulse from ZCD1 output terminals. The SHC1 output active power component iL(t) amplitude considered. A combined filtered load current error signals with band-pass filter BPF ψ included generated output multiplied with ρ power frequency signal. Later integration integral signal to the system and i_{Lpa} is evaluated which as particular phase 'A' measured load current. In similar way, the same progression is adapted for both phases 'B' and phase 'C' to extract final base load current components. Similarly, in order to get to excerpt reactive power components of iL1(t) basic fundamental load current for each phase-A or phase-B, phase-C with zero crossing detector ZCD2 used along with sinθ template pattern lag by 90° with cosθ template with the similar phase and trigger pulse attained at peak cosθ stencil templates. Second sample-and-hold circuit 2 SHC2 utilized with the input iL(t), trigger pulse from ZCD2 output. Then SHC2 output is reactive power component amplitude of load component iL(t). During the implementation process the k1, k2, and k3 values are used as 20, 10, and 2, correspondingly. By using three EPLL blocks estimated the reactive, active power components amplitudes of 3-phase load currents and their weighted averaged magnitudes are also used for estimation of load components.

The Load currents i_{Lpa}, i_{Lpb}, i_{Lpc} which are be an average of 3-Ø load active power components and riddled by means of Band pass filter (BPF) given as,

$$i_{LpA} = \left\{ \left(i_{Lap} + i_{Lbp} + i_{Lcp} \right) / 3 \right\} \tag{4}$$

In the same way, the load current [i_{Laq},i_{Lbq}, i_{Lcq}]3-phase reactive power components are take-out using with quadrature unit templates along with zero-crossed detector (ZCD2),sample and hold SHC2. These three quadrature load currents (i_{Laq}, i_{Lbq}, i_{Lcq}) are average value and cleaned filtered using with BPF to smoothen, compact the wrinkles, ripples in each current wave specified and given as

$$i_{LqA} = \left\{ \left(i_{Laq} + i_{Lbq} + i_{Lcq} \right) / 3 \right\} \tag{5}$$

3.2 EPLL frequency estimation and templates

The block diagram of Figure 5 explains the EPLL used for frequency estimation and each phase voltage templates with sin θ and cos θ. The vi(t) input signal to EPLL in order to provide and estimate SWECS frequency online with each phase sin, cosine templates. The error signal e(t) is the distortion signals are derived from the difference between vi(t) input sensed voltage and vL(t) estimated, sensed voltage basic fundamental component. The EPLL steadiness stability was analyzed that k1, k2, and k3 parameters control transient and along with the EPLL steady-state nature. The 3 block phase detector, loop filter, and voltage-controlled control oscillators used to estimate the frequency of each phase voltages at PCC and the sinθ template in phase with in-phase voltage phase component, meanwhile cosθ template headed forward, leads with each phase quadrature phase voltage components and by using three EPLLs these templates are estimated for each phase voltage independently to implement k1, k2, and k3 values chosen as 10, 5, and 5 respectively.

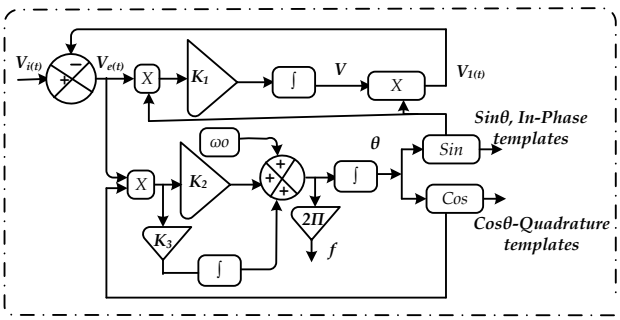

Figure 5. EPLL for frequency and phase voltage templates estimation

The unit templates of quadrature and In-phase components used to calculate compute the terminal voltage frequency which is given as in the following equation.

$$[w] = \left\{ \cos\theta \frac{d}{d\theta}\left(\sin\theta\right) - \sin\theta \frac{d}{d\theta}\left(\cos\theta\right) \right\} \tag{6}$$

$$where \sin\theta = w_{ap,} \cos\theta = w_{aq}$$

$$f = [w/(2\pi)] \tag{7}$$

The frequency (f_{err}) error measured, determined from the difference between the (f_{ref}) reference frequency and frequency (f) sensed above given as:

$$[f_{err}(n)] = \left\{ [f_{ref}(n)] - f(n) \right\} \tag{8}$$

Output frequency PI controller determined on nth sample instant given equation.

$$\begin{aligned} i_{fp}(n) = [& \{ i_{fp}(n-1) \} \\ & + k_{pf}\{ f_{err}(n) - f_{err}(n-1) \} \\ & + \{ k_{if} f_{err}(n) \}] \end{aligned} \tag{9}$$

where, proportional integral gains k_{pf}, k_{if} are acquired using optimization technique and the i_{spt} is total active component magnitude is evaluated with the sum of PI controller output i_{fp}, and i_{LpA} active load currents component and its average value magnitude is as:

$$[i_{spt}] = \{ i_{fp} + i_{LPA} \} \tag{10}$$

Measured(v_{te}) terminal voltage error is derived from the difference of (V_t) terminal voltage and (V_{tr}) reference terminal voltage at nth sample instant is as below equation.

$$[v_{te}(n)] = \{ [v_{tr}(n) - v_t(n)] \} \tag{11}$$

The voltage error (v_{te}) is allowed to pass to PI controller and it output voltage, quadrature current component (i_{vq}) at nth sample instant arithmetically as:

$$\begin{aligned} [i_{vq}(n)] = [& i_{vq}(n-1) + k_{pv}\{ v_{te}(n) - v_{te}(n-1) \} \\ & + k_{iv} v_{te}(n)] \end{aligned} \tag{12}$$

The (i_{sqt}) total reactive current magnitude evaluated, calculated from (i_{LqA}) average reactive currents and (i_{vq}) PI controller output voltage is written as

$$[i_{sqt}] = \{ I_{vq} + I_{LqA} \} \tag{13}$$

3.3 The estimation of active and reactive power component amplitude of reference source currents

The source reference active power current components predictable and derived from the difference or sum of two components of PI controller frequency output (I_{fp}) and weighted load current active power component average amplitude in Eq. (10). In order to obtain the frequency error which is calculated and evaluated from the two components are reference frequency f_{rf} and "f" SWECS estimated terminal voltages frequency and (f) is estimated by EPLL in Eq. (8) at n^{th} sampling instant.

The reference source reactive power component currents are obtained and determined from the difference of the two components are weighted average load current reactive power component amplitude and the PI controller output voltage component are used in Eq. (13) and at nth sampling instant the AC voltage error v_{te} is estimated from the difference of V_{tr}(t)

is AC reference phase terminal voltage magnitude, $V_t(t)$ detected 3 phase ac voltage amplitude on PCC computed from equation (11). At nth sampling instant PI controller PI gains k_{pv}. k_{iv} are obtained as constants from PI regulator voltage output to maintaining the ac terminal voltage constant. $V_e(t)$ and $V_e(t-1)$ voltage error at n^{th}, $(n-1)^{th}$ sample instant respectively and $I_{vq}(t)$, $I_{vq}(t-1)$ PI regulator voltage output at n^{th}, $(n-1)^{th}$ instantaneous rewardingly necessary to control voltage.

3.4 EPLL to estimation of reference source currents

The 3-phase source reference active power current component are computed by phase and their amplitude templates $\sin\theta_a$, $\sin\theta_b$, and $\sin\theta_c$ are in-phase for all three phases a, b, and c, respectively in Eq. (14) and the 3-phase reference source reactive power current component quadrature templates phase and amplitudes are $\cos\theta_a$, $\cos\theta_b$ and $\cos\theta_c$ are for 3 phases A, B, and C, respectively in Eq. (15). The amplitude of 3-Ø active and reactive reference source currents are given as

$$\begin{aligned}(i_{sap}) &= [i_{spt} * \sin\theta_{pa}] \\ (i_{sbp}) &= [i_{spt} * \sin\theta_{pb}] \\ (i_{scp}) &= [i_{spt} * \sin\theta_{pc}]\end{aligned} \tag{14}$$

$$\begin{aligned}(i_{saq}) &= [i_{sqt} * \cos\theta_{qa}] \\ (i_{sbq}) &= [i_{sqt} * \cos\theta_{qb}] \\ (i_{scq}) &= [i_{sqt} * \cos\theta_{qc}]\end{aligned} \tag{15}$$

The estimated reference source currents are:

$$\begin{aligned}[(i^*_{sa})] &= [i_{sap} + i_{saq}] \\ [(i^*_{sb})] &= [i_{sbp} + i_{sbq}] \\ [(i^*_{sc})] &= [i_{scp} + i_{scq}]\end{aligned} \tag{16}$$

From the Eq. (16) these 3-phase reference source current (i_{sa}, i_{sb}, i_{sc}) evaluated and matched with detected with 10 kHz frequency triangular amplitude source current (i^*_{sa}, i^*_{sb}, i^*_{sc}) and detected source current errors utilized to create and produce gating pulse to IGBT switches first three legs VSC.

3.5 The neutral currents compensation

The three leg VSC activated, used for compensation of source neutral current and zero sequence currents couldn't pass to ac delta capacitors. In order to accomplish this, (i_{sn}) source neutral wire current is detected and equated with neutral reference current value ($i^*_{sn} = 0$). The net error current used to produce switching pulse to IGBT three leg VSC.

4. SYSTEM DESIGN

The proposed Design and modeled SWECS be made up of a wind turbine generator set, Zigzag transformer, delta connected Capacitor, VSC and a VFC consists of 3 leg IGBT based VSC, BESS with 3–Ø4-wire customer loads are allowed in MATLAB/Simulink with simpower model evaluated the system performance within the optimal limits. Every first 3 legs midpoint associated with each specific phase A, B and C at PCC along through ac interface inductors with delta connected excitation capacitors along with zigzag transformer connected for the load current neutral terminal and a 7.5 kW IG based SWECS. The control algorithm comprehended in MATLAB setting used with the switching signal to IGBT VSC control algorithm.

4.1 The turbine modeling

The power extracting mechanism is made available with the wind turbine which output mechanical power, torque are Pwt, Twt according to Betz theory, is function of the rotor speed with various wind speed and its optimum maximum power captured from random wind if the controller can properly operate. The derived mechanical output power in per unit system developed with wind turbine generator technology with following equation.

$$P_m = 0.5 * C_p * A * v_w^3 \tag{17}$$

Here, Power coefficient=C_p, wind speed = v_w, mechanical power output = P_m, A blade swept area, $C_p(\lambda, \beta)$ power coefficient which determined function of the 'λ','β'tip speed ratio, pitch angle respectively as following equation.

$$c_p(\lambda,\beta) = c_1\left(\frac{c_2}{\lambda_1} - c_3 - c_4\right)e^{c6/\lambda^1} + c_6\lambda \tag{18}$$

$$\frac{1}{\lambda} = \frac{1}{\lambda + 0.008\beta} - \frac{0.038}{\beta^3 + 1} \tag{19}$$

Figure 2 shows the plot the curve of wind turbine output with different wind speed along with zero pitch angle (β).

4.2 The battery storage system modeling

Battery Energy Storage System (BESS) is the most important storage element used in today's power system in order to give solutions for the different operational problems which we are facing. In present generation the fast responsive electronic devices with BESS has providing additional wide range applications in power system than the past traditionally method to control, maintain the regulation, protection, power factor correction, load management, balancing and enhancing system reliability and improved the power quality issues. The battery bank storage capacity for SWECS is based on wind speed at particular location and connected consumer loads. The battery bank selecting with maximum, large size to facilitate best contingency load leveling, handling than the lesser battery bank capacity even though with similar time period, space, increased early speculation, regular maintenance problems. Therefore, battery bank storage capacity selection is based on capacitance C_b, as well as on above mentioned all aspects which are considered for required $V_{dc}$is greater than the 376 V and with minimum battery voltage 420 V and Battery dc bus voltage derived using the following equation.

$$[V_b] = \left\{ \frac{\left(2\sqrt{2}\right)V_{ph}}{m} \right\} \quad (20)$$

The battery model equivalent circuit is symbolized as both capacitor (C_b) and (R_b) resistance are connected in parallel the combination is in series with resistance (Rs) connected and battery voltage (V_b) with internal resistance for self-discharging, battery energy in kWh and C_b= capacitance will be calculated by below equation:

$$[C_b] = \left\{ \frac{kWh * 3600 * 10^3}{0.5\left(V_{\max}^2 - V_{\min}^2\right)} \right\} \quad (21)$$

where, V_{max}, V_{min} values are battery voltages, where v_{oc}min and v_{oc}max are open circuit battery voltages during full discharged, charged situations and its units in kilo-watt hours kWh directly proportional to C_b. In order to proper operation and implementation, the battery rack with 2.9 kWh capacities used to power storage. The 12-V, 7-Ah 35 units storage used in series configuration for minimal battery dc bus voltage 420 V and for maintain the maximum v_{oc}max, minimum v_{oc}min open-circuit battery voltages 472.5 V, 367.5 V correspondingly and obtained C_b value is 236.73 Farads which is same as the battery storage value which is used in implementation.

4.3 The filtering ac interface inductor design

The permissible, sharp acceptable (i_{pp})peak–peak ripple current, (V_{dc})dc bus voltage as V_b, and (f_m) modulating switched frequency of VSC functions are used in selection of an AC designed filtering inductor (L_f). Therefore, the L_f is calculated as:

$$[L_f] = \sqrt{3}\, m V_b / (12\, a\, f_m\, i_{pp}) \quad (22)$$

where, modulation index (m) and overloading factor (a) considering m = 1 underneath poorest case, selected battery dc-link voltage V_{dc}, V_b = 420 V, a = 1.3 or 1.2, i_{pp} peak–peak VSC ripple current i_{pp} = 5% or10% of the VSC current and f_m switching frequency of VSC, f_m= 10 kHz, L_f = 2.2 mH.

Based on input wind speed the VSC deliveries or absorbs active, reactive powers which are connected different consumer loads. Under worst case when the load is not coupled on PCC, the VSC taking rated generated power when IG needs reactive power demand 140%–160% is 5.9 kVAR to supply rated power to consumers for which 8-kvar capacitor bank coupled with IG terminals and VSC desires to deliver shortage, insufficiency 1.9 kVAr reactive power to IG bus. Hence, VSC rating determined as Svsc = Square root of P^2 + Q^2 = 37002 + 19002 = 4.159 kVA and VSC per phase current calculated Svsc= √ 3VLIvsc and VSC obtained current is 10.44 A, and ipp is 1.04 A. The Lf value is determined as 4.48 mH, around 4 mH selected nearer to designed values.

4.4 Design of star-delta transformer

Figure 6 shows the zig-zag transformer and phasor diagram and its winding voltages values V_{a1}=V_{b1}=V_{c1}=V_{a2}=V_{b2}=V_{c2} presented as voltages per winding, considering [V_a = V_b = V_c] = V resultant voltage. If the line to line voltage value V_{ab} = 415 V, phase voltages V_a = V_b = V_c = 415/√3 = 239.6 V, V_{a1} = V_{b1} = V_{c1} = V_{a2} = V_{b2} = V_{c2} = 138.3 V and V_{a3} = V_{b3} = V_{c3} = 138.3 V respectively taken.

The neutral current compensation was done by 5 kVA rating zigzag transformer, which also reduces the battery voltage. The primary winding voltage per phase is:

$$v_{AN} = (v_{LL}/\sqrt{3}) = 239.6V = 415/\sqrt{3} \quad (23)$$

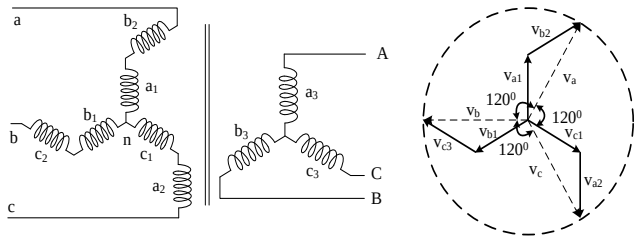

Figure 6. Transformer (zigzag-star) and phasor diagram

5. OPTIMIZATION TECHNIQUES

In order to obtain the optimal tuned PI controller gain parameters is a great challenge for which a meta-heuristic techniques are proposed and investigated to deal with the revealed in adequacies and insufficiencies with optimized control structure as per the best author's knowledge has been employed to improve VSC response within SWECS and dynamic Matlab simulations model developed as per the advantages of given optimization techniques which are used to diminish PI controller errors and to produce determine optimized PI controller gains which are prime most important and effective operational dynamics of SWECS and enhanced power quality. ISTE Integral Time weighted Squared Error Cost function of optimization problem of decreasing steady state error PI1 and PI2 as shown below:

$$[CF] = [w_1 * ISTE_1 + w_2 * ISTE_2] \quad (24)$$

where, $ISTE_1$, $ISTE_2$ are the input errors of terminal voltage and frequency PI controllers taken from Eqns. (8) and (11).

$$Cost\ Function = w_1 \left\{ f_{err(n)} \right\} + w_2 \left\{ V_{te(n)} \right\} \quad (25)$$

5.1 Particle Swarm Optimization (PSO)

Figure 7 shows the flow chart of algorithm of PSO, which is executed to acquire optimized frequency (f) and terminal voltage (V_t) controllers gains.

Figure 8 (a) shows the trajectory of gains k_{pf}, k_{if} of frequency PI controller and values are establish, found to be K_{i1}=5 & K_{p1} = 5. Figure 8 (b) shows the trajectory of AC voltage PI controller gains k_{pv}, k_{iv} of acquired values are K_{i2}=3.77, K_{p2}=1.38 and Figure 8 (c) shows the convergence curve and settled value 14.58 in 2nd iteration using PSO technique.

Table 1 shows the optimum PI gains using PSO algorithms technique realistic and furnished.

Table 1. PI gains with PSO algorithms

Gains / Algorithm	Frequency PI gains		Voltage PI gains		Convergence of Cost function	Comments
	K_{pf}	K_{if}	K_{pv}	K_{iv}		
PSO	5	5	1.38	3.77	14.58	mostly suited for the system

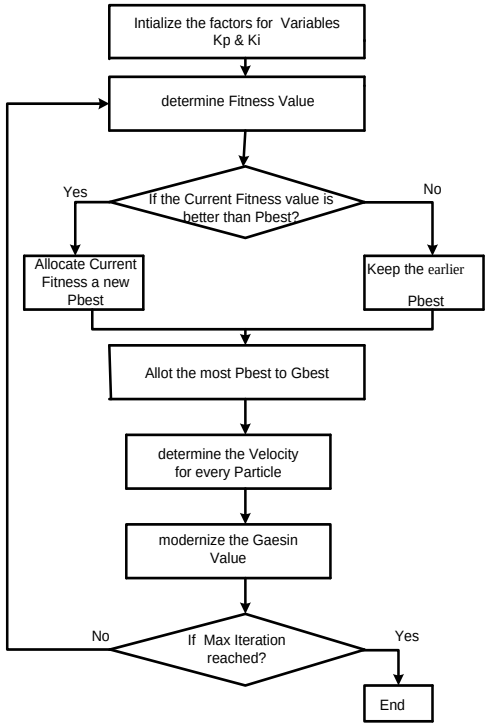

Figure 7. PSO algorithm flowchart for optimum PI gains

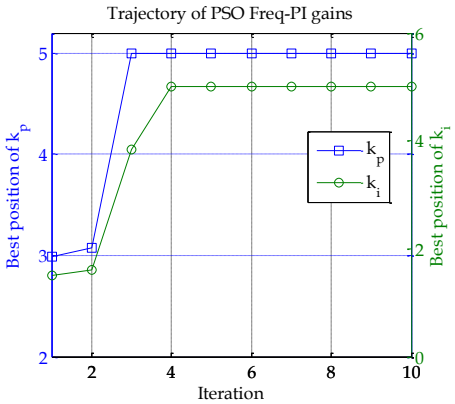

(a) Optimized Frequency -PI gains

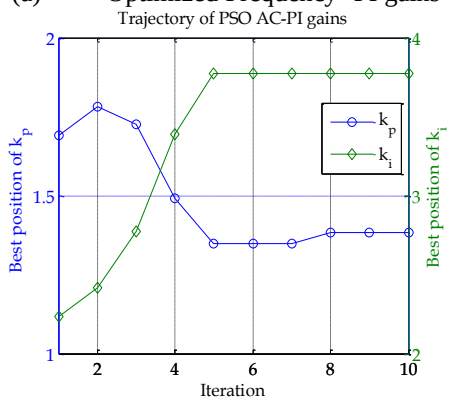

(b) Optimized AC-PI gains

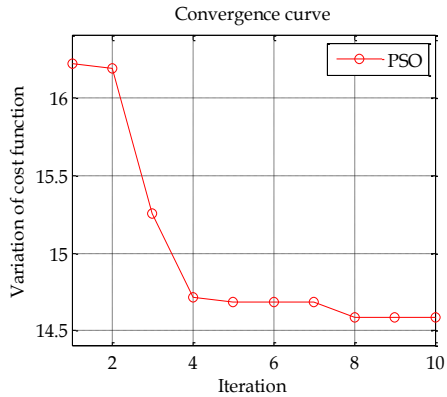

(c) PSO-Convergence curve

Figure 8. Algorithm PSO - PI gains and convergence Trajectory curve

6. RESULTS AND DISCUSSION

The different consumer's loads like domestic lights, pumping water, heating purpose, testing equipment application, boring and drilling applications are feeding by the proposed, developed IG-based remote area autonomous SWECS and these various loads categorized linear, nonlinear, dynamic loads as SQIM driven along through solid state controlled variable-speed drives nowadays with good energy efficient and behaves as nonlinear loads. The performance of IG-based SWECS test results are presented without switching the VFC and thereafter presented, demonstrated the VFC performance with balanced, unbalanced nonlinear load which are most severe to the controller. The EPLL control algorithm optimal PI gains are obtained, applied and used for modeled and designed 7.5 kW capacity rating, 50 Hz SWECS wind turbine driven IG set was examined and test results are verified tabulated for 3-Ø 4 wire various linear, non-linear load.

The following Figures 9 and 10 characterizes the various linear, non-linear load waveforms for stubborn wind speed throughout the 7.64 sec to 7.76 sec and the results are recorded and those waveforms are explained in terms of electrical terminology as a v_s generator source voltage, is generator source current, different consumer load current-$i_{L,\,ic}$ controller current, generated power-P_g, battery power P_b, and consumer load power-PL, V_t terminal voltage, v_b battery voltage, i_b battery current, i_{sn} source neutral wire terminal current, i_{Ln} load neutral terminal current, frequency are provided and explained in below sections.

6.1 Performance of controller with linear loads

Three phase diode bridge rectifiers through circuit breaker connected with resistive linear loads for study VFC performance as voltage regulator device, harmonic eradication

and load balancing. The controller steady state presentation and examined simulation results are recorded as 3-phase generator ripple free currents and balanced values. The excitation capacitor currents detected along VSC switching ripples with V_b demonstrated and the VSC currents contain less active power component which is a difference of generator power and load power, the reactive power components for voltage regulating and the load neutral wire current passing through zigzag transformer neutral path terminal. Generator current and voltage values THD's percentage within IEEE-519 boundaries.

The Figure 9 enlightens, described regarding various waveforms during time period 7.6 sec to 7.64 sec and 7.74 sec to 7.8 sec for the SWECS designed model with linear consumer loads. The 9 kW rated capacity generator deliveries 7.5 kW to consumer loads and remaining 1.5 kW power stored battery which will be given back or delivered back to the loads whenever it needed under discharging mode as a negative battery current. The 3 kW load on one phase, if 'A' is taken off by turning off the circuit breaker at 7.64 sec and at 7.76 sec connected back by closing the same breaker when the battery is charging which indicates battery current positive (+ve) due to the surplus power during same period and 3-phase source current i_{sa}, i_{sb}, i_{sc} same detected with balanced loads even during unbalanced loads. The During the whole operation time the generator source currents are absolutely balanced by controller injection currents, therefore obtaining the load level balancing and system balanced. During unbalance condition the consumer's load currents I_{la}, neutral load current I_{ln} are expressed with I_{sn} zero source neutral current negligible and abolished neutralized the load neutral current by zigzag transformer known as neutral path current compensation. While the transient condition, uneven normal linear load state the SWECS frequency monitored, supervised at 50 Hz frequency constantly and its terminal voltage (V_t) is regulated, monitored at 415 V voltage which is verified, observed, referred as constant voltage regulation of SWECS.

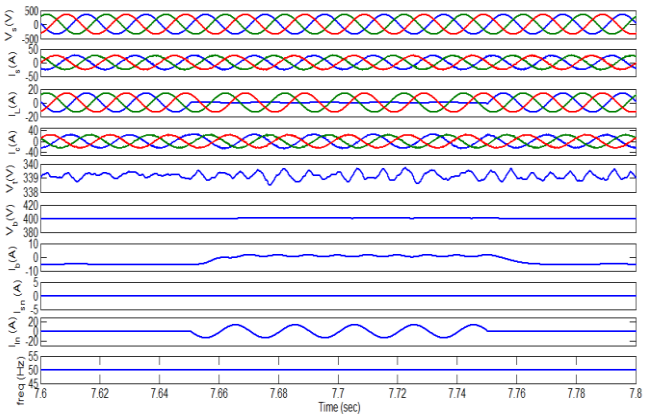

Figure 9. Performance with linear load waveforms

6.2 Performance of controller with non-linear loads

Nowadays due to enlarged expanded utilizing power electronics, power converter, handled power resource on different application like instrumentation, varying speed drives, energy efficient lights etc., all of these loads pull nonlinear currents from source supply. For which it is good to verify the VFC operation with any non-linear load. The VFC operated along with the 3 phase 8.7 kW diode bridge rectifier with resistive-inductive non-linear load coupled to circuit breaker and dc link in SWECS for voltage regulation, distortion eradication and load leveler.

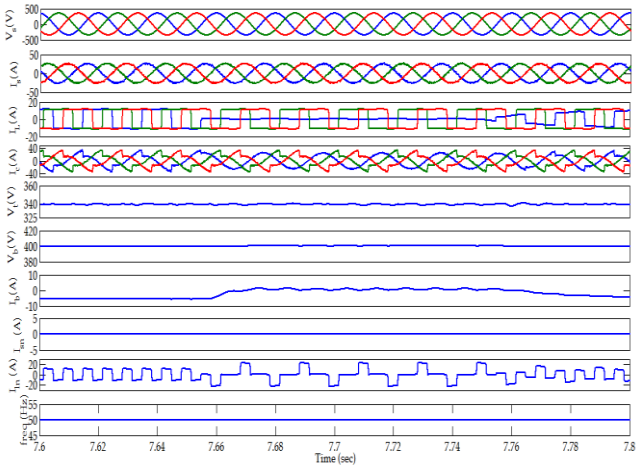

Figure 10. Performance waveforms with Non-linear loads

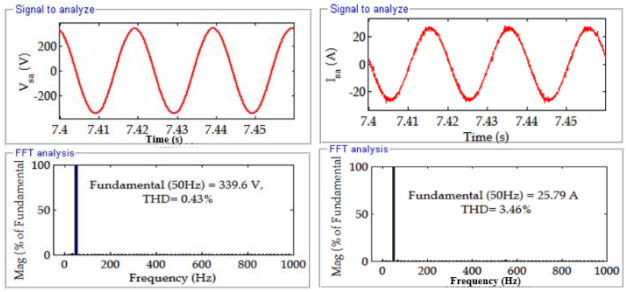

(a) %THD of Source voltage, (b) %THD of Source current

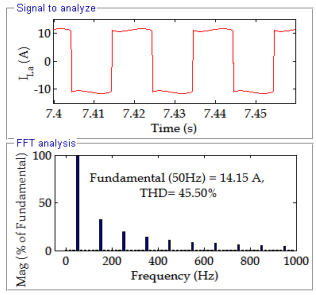

(c) %THD of Load current

Figure 11. Waveforms and harmonic spectrum

Figure 10 describes the proposed system various components waveforms of with inductive load and the controller steady state values are furnished and simulated results recorded as a balanced ripple free source currents and the excitation capacitor currents with VSC switching ripples with 3-phase nonlinear consumers load currents and these VSC currents contains active power component and supplies reactive power component for the purpose of terminal voltage regulation and VSC absorbs the excesses surplus generated power to control the SWECS frequency and for harmonics compensation. The load neutral current passing through zigzag transformer and finally the Pg generator power, P_L load power and P_b battery charging power labeled. System any phase if "A' 'load is switched off at 7.64 sec and reconnected at 7.76 sec by operating the same breaker, an input power to IG is same as in prior condition, source currents maintained, observed similar with balanced load even though consumers loads unbalanced condition without harmonic which are free due to controller injected currents and the zigzag transformer

used to balance the distorted currents, compensate both consumer neutral path current, source neutral currents with significantly zero value.

In both balanced & unbalanced conditions, positive(+ve) I_b battery current indicates charging mode when the battery stores excess power during generation power greater than the consumers load demand and the negative (–ve) battery current signifies discharging mode dispenses or delivers the consumer's deficit power when generation power lesser than the consumer's load power. During operation period from 7.6 sec to 7.82 sec proposed system terminal voltage V_t and if frequency (f) is synchronized obtained as 415 V and 50 Hz which are regulated and maintained constant whole SWECS operation.

The Figure 11 (a) to (c) explains and informs us regarding source voltage, current and load current magnitude along with various harmonic waveforms spectrum with measured 0.43% THD source voltage, 3.46% THD source current and 45.50%. THD load current. As per the IEEE-519 standards and those parameters values are acceptable and worthy with optimal limits.

7. CONCLUSION

The proposed designed model execution of three-leg VSC, SWECS with storage element has carried out for the 3-phase 4 wire remote system and Simulation results have been revealed confirmed the EPLL acceptable, satisfactory steady-state and dynamic performance based VFC control algorithm utilized to control voltage, frequency and also to generate estimated reference source current components very fast under balanced/unbalanced conditions with improved system power quality concerns for controller with predictable quadrature, in-phase components of load currents unit templates of SWECS and EPLL inherent feature is to estimate the system frequency quickly with expected optimal gains with reduced computation burden and PI controller's two gains are optimized by means of PSO fulfilled fitness values and the compared the previous results of trajectory of terminal voltage and frequency with PSO compared with previous ALO and DOA techniques gains in the revised manuscript and the limitation of the this study id 3leg, 4leg VSC of SWECS with IG with fixed wind speed 10m/s, power supply to the remote consumer loads. The zigzag transformer operated for neutral path current compensation, based on gained test results accomplishes EPLL battery based VFC system performance is efficient and giving the optimal operational functions of load leveling load balancing, harmonic reduction and a neutral wire current compensator. The Simulated results are revealed, appraised, recognized and achieved in whole system operation without any delay.

REFERENCES

[1] Chishti, F., Murshid, S., Singh, B. (2020). Unbiased circular leakage centered adaptive filtering control for power quality improvement of wind-solar PV energy conversion system. IEEE Trans. Sustain. Energy, 11(3): 1347-1357. https://doi.org/10.1109/TSTE.2019.2925089

[2] Amin, M.M.N., Mohammed, O.A. (2010). Power quality improvement of grid-connected wind energy conversion system for optimum utilization of variable speed wind turbines. IECON 2010 – 36th Annual Conference on IEEE Industrial Electronics Society, pp 3287-3292. https://doi.org/10.1109/IECON.2010.5675336

[3] Mendis, N., Muttaqi, K.M., Sayeef, S., Perera, S. (2012). Standalone operation of wind turbine-based variable speed generators with maximum power extraction capability. IEEE Trans. Energy Convers., 27(4): 822-834. https://doi.org/10.1109/TEC.2012.2206594

[4] Moradian, M., Soltani, J. (2016). An isolated three-phase induction generator system with dual stator winding sets under unbalanced load condition. IEEE Trans. Energy Convers., 31(2): 531-539. https://doi.org/10.1109/TEC.2015.2508958

[5] Bouchiba, N., Barkia, A., Sallem, S., Chrifi-Alaoui, L., Drid, S., Kammoun, M. (2017). A real-time Backstepping control strategy for a doubly fed induction generator based wind energy conversion system. 2017 6th Int. Conf. Syst. Control., pp. 549-554. https://doi.org/10.1109/ICoSC.2017.7958744

[6] Gowtham, N., Shankar, S., Rao, K. (2017). Enhanced firefly algorithm for PQ improvement of wind energy conversion system with UPQC. TENCON 2017 - 2017 IEEE Region 10 Conference, pp. 757-762.

[7] Amin, M.M., Mohammed, O.A. (2011). Development of high-performance grid-connected wind energy conversion system for optimum utilization of variable speed wind turbines. IEEE Trans. Sustain. Energy, 2(3): 235-245. https://doi.org/10.1109/TSTE.2011.2150251

[8] Puchalapalli, S., Singh, B. (2020). A novel control scheme for wind turbine driven DFIG interfaced to utility grid. IEEE Trans. Ind. Appl., 56(3): 2925-2937. https://doi.org/10.1109/TIA.2020.2969400

[9] Rezkallah, M., Chandra, A., Singh, B., El Kahel, M. (2012). Vector control of squirrel-cage induction generator for stand-alone wind power generation. IECON Proc. (Industrial Electron. Conf.), pp. 1166-1171. https://doi.org/10.1109/IECON.2012.6388607

[10] Xu, G., Xu, L., Morrow, D.J., Chen, D. (2012). Coordinated DC voltage control of wind turbine with embedded energy storage system. IEEE Trans. Energy Convers., 27(4): 1036-1045. https://doi.org/10.1109/TEC.2012.2220361

[11] Wang, Z., Zheng, Y., Cheng, M., Fan, S. (2012). Unified control for a wind turbine-superconducting magnetic energy storage hybrid system based on current source converters. IEEE Trans. Magn., 48(11): 3973-3976. https://doi.org/10.1109/TMAG.2012.2201213

[12] Singh, B., Rajagopal, V. (2009). Battery energy storage based voltage and frequency controller for isolated pico hydro systems. J. Power Electron., 9(6): 874-883.

[13] Sharma, S., Singh, B. (2014). Asynchronous generator with battery storage for standalone wind energy conversion system. IEEE Trans. Ind. Appl., 50(4): 2760-2767. https://doi.org/10.1109/TIA.2013.2295475

[14] Ammar, M., Joós, G. (2014). A short-term energy storage system for voltage quality improvement in distributed wind power. IEEE Trans. Energy Convers., 29(4): 997-1007. https://doi.org/10.1109/TEC.2014.2360071

[15] Karbouj, H., Rather, Z.H. (2019). A novel wind farm control strategy to mitigate voltage dip induced frequency excursion. IEEE Trans. Sustain. Energy, 10(2): 637-645. https://doi.org/10.1109/TSTE.2018.2842232

[16] Tanaka, T., Wang, H., Blaabjerg, F. (2019). A DC-link capacitor voltage ripple reduction method for a modular

multilevel cascade converter with single delta bridge cells. IEEE Trans. Ind. Appl., 55(6): 6115-6126. https://doi.org/10.1109/TIA.2019.2934024
[17] Kasal, G.K., Singh, B. (2008). VSC with zig-zag transformer based decoupled controller for a pico hydro power generation. Proc. INDICON 2008 IEEE Conf. Exhib. Control. Commun. Autom., 2: 441-446. https://doi.org/10.1109/indcon.2008.4768764
[18] Sharma, S., Singh, B. (2011). An enhanced phase locked loop technique for voltage and frequency control of stand-alone wind energy conversion system. India Int. Conf. Power Electron. IICPE, pp. 1-6. https://doi.org/10.1109/IICPE.2011.5728064
[19] Sexon, B.A. (1980). Wind turbines. Phys. Technol., 11(5): 196-197. https://doi.org/10.1088/0305-4624/11/5/407
[20] Sun, K., Yao, W., Fang, J., Ai, X., Wen, J., Cheng, S. (2020). Impedance modeling and stability analysis of grid-connected DFIG-based wind farm with a VSC-HVDC. IEEE J. Emerg. Sel. Top. Power Electron., 8(2): 1375-1390. https://doi.org/10.1109/JESTPE.2019.2901747
[21] Sharaf, A.M., El-Gammal, A.A.A. (2009). Optimal energy utilization for a stand-alone wind energy scheme WES. 2009 IEEE Electr. Power Energy Conf., pp. 1-6. https://doi.org/10.1109/EPEC.2009.5420884
[22] Raza, A., Yousaf, Z., Jamil, M., et al., (2018). Multi-objective optimization of VSC stations in multi-terminal VSC-HVDC grids, based on PSO. IEEE Access, 6: 62995-63004. https://doi.org/10.1109/ACCESS.2018.2875972
[23] Singh, B., Rajagopal, V. (2011). Neural-network-based integrated electronic load controller for isolated asynchronous generators in small hydro generation. IEEE Trans. Ind. Electron., 58(9): 4264-4274. https://doi.org/10.1109/TIE.2010.2102313
[24] Assiri, A.S., Hussien, A.G., Amin, M. (2020). Ant lion optimization: Variants, hybrids, and applications. IEEE Access, 8: 77746-77764. https://doi.org/10.1109/ACCESS.2020.2990338
[25] Bo, H., Niu, X., Wang, J. (2019). Wind speed forecasting system based on the variational mode decomposition strategy and immune selection multi-objective dragonfly optimization algorithm. IEEE Access, 7: 178063-178081. https://doi.org/10.1109/ACCESS.2019.2957062
[26] Singh, B., Arya, S.R. (2013). Implementation of single-phase enhanced phase-locked loop-based control algorithm for three-phase DSTATCOM. IEEE Transactions on Power Delivery, 28(3): 1516-1524. https://doi.org/10.1109/TPWRD.2013.2257876

APPENDIX

WECS Data: 4-pole, 50 Hz, 415 V, 7.5 kW Star-Connected IG with a stator resistance is 1 Ω, stator inductance is 0.00478 H, rotor inductance 0.00478 H, rotor resistance 0.77 Ω and mutual inductance 0.334 H.

Wind Turbine Data: C_{pmax}=0.48, λm =8.1, 7.5 kW, C1 =0.5176, C2=116, C3=0.4, C4=5, C5=21, C6=0.0068, C7=0.008, C8=0.035.